Proceedings of the ASME 2020 15th International Manufacturing Science and Engineering Conference MSEC2020 September 3, 2020, Virtual, Online

MSEC2020-8444

NUMERICAL INVESTIGATION OF VARIOUS COAXIAL NOZZLE DESIGNS FOR DIRECT LASER DEPOSITION

Theodore T. Gabor, Hang-Eun Joe, Semih Akin, Martin Byung-Guk Jun*
Jun Laboratory
Department of Mechanical Engineering
Purdue University
West Lafayette, Indiana 47906
Email: mbgjun@purdue.edu

Kyung-Han Kim, Jong-Kwon Park
Advanced Manufacturing Systems Research Division
Korean Institute of Machinery and Materials
Yuseong-Gu, Daejeon, 34103
South Korea
khkim@kimm.re.kr
jkpark@kimm.re.kr

ABSTRACT

Direct Laser Deposition (DLD) is a form of metal-based additive manufacturing. The DLD process involves ejecting powder out of a nozzle by means of an compressed gas and irradiating a laser beam to heat up the powder and the substrate. During the powder spray ejection, tight focusing of the powder stream has the potential to improve the DLD process by reducing powder wastage. Thus, nozzle design and computational fluid dynamics (CFD) analysis of the design parameters become important. This study focuses on the numerical simulation of the gas-solid flow inside a coaxial DLD nozzle and how design features of the nozzle affect powder focusing. The two-phase gas/powder flow was analyzed using a Eulerian-Lagrangian scheme. A total of twelve designs were simulated and analyzed through CFD simulation, with features such as inlet angle, inlet offset, and the presence and shape of flow-straightening grooves considered. It was determined that geometry reducing particle tangential velocity such as flow-straightening grooves produce the best focusing effects, whereas offset inlets without the presence of grooves reduces focusing by maximizing particle swirling. Finally, the simulations show that the distribution of powders within the nozzle is also affected by nozzle inlet angle, with horizontal inlets providing more even distribution over inlets angled towards the nozzle tip.

*Address all correspondence to this author.

1 Introduction

Direct Laser Deposition (DLD) is a laser-based additive manufacturing (AM) process that has potentials to be used and widely adopted in manufacturing industries. The DLD process involves ejecting powder out of a nozzle by means of an compressed gas and irradiating a laser beam to heat up the powder and the substrate. By heating up powder and substrate, a melt pool develops, allowing the substrate and powder to fuse into a single material before it is cooled down. Compared to other additive manufacturing methods, such as selective laser sintering (SLS) and selective laser melting (SLM), the DLD process uses the nozzle for ejecting powder instead of a bulk powder bed. As the nozzle has more compact form, it can be mounted to a gantry or robot, which allows more precise manufacturing control and decreases production time. A coaxial or a radially symmetric design of the nozzle has generally used in DLD technique because it has the unique potential of even powder distribution. It is important to note that the DLD technique has many other names, such as laser direct casting, laser cladding, and laser engineered net shaping (LENS), although some of these terms can also be used to refer to a specific patented design (e.g. LENS). [1, 2, 3].

Coaxial nozzle design is required to be determined by considering the physical processes of the DLD technique. The processes are generally categorized into the melt pool process, the powder stream process, and the characterization of material properties [3]. The powder stream process is mainly considered

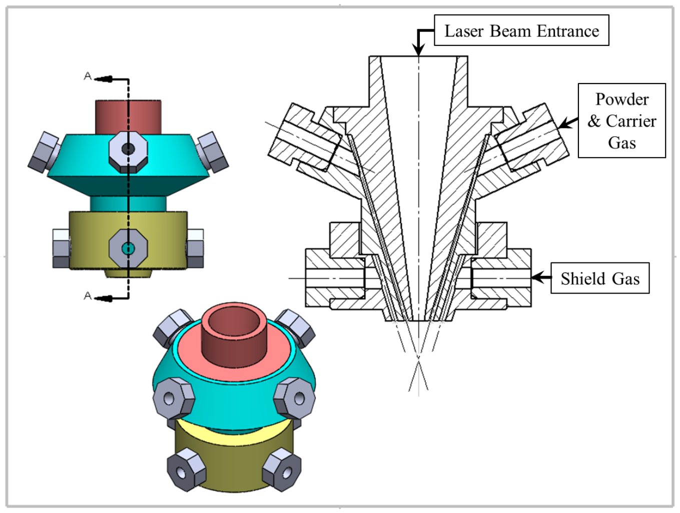

FIGURE 1. ILLUSTRATION OF NOZZLE GEOMETRY WITH BOTH POWDER/CARRIER GAS INLETS AND SHIELD GAS INLETS.

to design the coaxial nozzle for DLD. The powder stream process encompasses the flow of powder and carrier/shield gas inside the nozzle, the flow of powder and carrier/shield gas out of the nozzle, and the interaction between the ejected powder particles and the laser. The trajectory of the powders ejected from the coaxial DLD nozzle is affected by the flow conditions set within the nozzle itself and the geometric designs of the nozzle can also affect the flow.

There are numerous theoretical modeling studies devoted to understanding the various physical processes of the DLD technique. Computational fluid dynamics (CFD) is typically used for powder flow and nozzle design because it enables to analyze two-phase flow of gas and particles as it can take into account the geometry of the nozzle and the boundary conditions (e.g. ambient pressure, powder feed rate, carrier/shield gas volumetric flow rate, etc.). The most common model used for DLD nozzle design is an Eulerian-Lagrangian CFD model [4]. Wen et al. [5] used it to analyze not only the particle trajectories exiting the nozzle, but also thermodynamics of the powder as it is heated up by the laser, although the nozzle was simulated as a simpler 2-D axisymmetric model. Tabernero et al. [6] studied the flow of a coaxial nozzle with a honeycomb flow straightener and characterized the concentration of powder evolved within the ejected stream.In another paper, Tabernero et al. [7] documented the design process of a coaxial nozzle and determined that grooves can straighten a powder flow and improve powder focusing. However, the authors do not explore how the shape of the grooves or other major design features affect nozzle focusing and powder distribution within the nozzle.

In addition, the coaxial nozzle was simulated with powder hitting the substrate below. Ibarra-Medina and Pinkerton [8] also simulated the flow of the powders within a coaxial nozzle as well as the ejected powders on the substrate. It was found that the powder concentration within the coaxial nozzle is not completely coaxial, with the concentration the highest in locations corresponding to the powder inlets. The second is that the powders will impact the inner wall of the nozzle, then bounce between the two walls as the powder spreads out, gradually gaining acceleration as it goes through the nozzle.

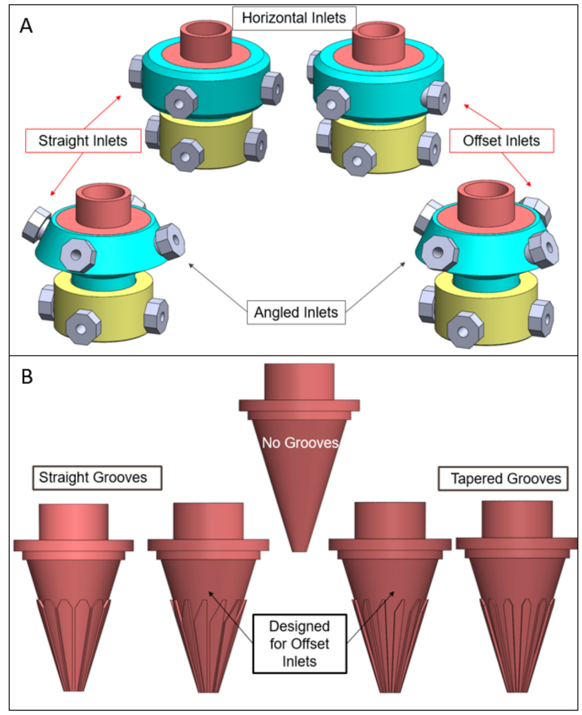

FIGURE 2. VISUAL OF THE DIFFERENT DESIGN VARIATIONS FOR (A) INLET CONFIGURATION,(B) FLOW-STRAIGHTENING GROOVE DESIGN.

In this study, several designs of coaxial nozzles are studied to determine which design parameters produce the best focusing within a coaxial nozzle. The inlet angle, inlet offset, and the presence and shape of flow-straightening grooves were considered to design the coaxial DLD nozzle. Each combination of these design features was analyzed using Eulerian-Lagrangian CFD model at different inlet conditions. Moreover, a full factorial design of experiment (DOE) is coupled with the CFD simulation results to determine the effect and contribution of design parameters on powder stream focusing.

2 Modeling Overview

2.1 Nozzle Design and Simulated Fluid Region

Although designs between different coaxial DLD nozzles vary, there are still several design similarities throughout. First,

TABLE 1. MATERIAL PROPERTIES FOR BOTH THE GAS PHASE AND THE METAL POWDERS.

Gas Material	Gas Density (kg/m^3)	Gas Viscosity ($kg/(m \cdot s)$)	Powder Material	Powder Density (kg/m^3)	Min. Diameter (μm)	Max Diameter (μm)	Average Diameter (μm)	Spread Parameter	Number of Diameters
Argon	1.6228	2.125e-5	Steel	8030	15	50	32.5	3.5	10

there is always a nozzle in which the powder is delivered to the substrate by gas flow, usually via a nonreactive gas such as argon. This section of the nozzle is always a region of two-phase flow, where the metal powder particles and the carrier gas interact. In addition, this region is always angled inward towards the centerline (although the angles vary between different nozzles), which helps the particles focus within a particular region. Again, the focus region varies based on the geometry of the nozzle. Secondly, all coaxial nozzles have discrete inlets for the particles to enter the nozzle. As shown by Ibarra-Medina et al. [8], this means that the particles are not evenly distributed within the nozzle, which can affect particle concentration at the focus region. Although there can be changes to the design that can ensure a more even particle distribution, those features are not common to this design. Finally, all coaxial nozzles have a central opening within the nozzle to allow the laser to hit the ejected particle cloud and substrate below unimpeded by the nozzle. This clearance necessitates the nozzle to be angled inwards, but allows the powder to be evenly hit by the laser beam as long as the nozzle has a good enough powder distribution within the nozzle.

In addition to these features, there have also been other common features in coaxial nozzles that help with the cladding process. Many nozzles also supply shield gas on the inside or outside of the powder nozzle, which ensures that the powder and substrate do not oxidize when they absorb heat from the high powered laser. To ensure a more even particle distribution within the nozzle, different nozzle designs may also combine offset inlets with flow-straightening geometry. Offsetting the inlets forces the particles to swirl around in the upper chamber of the nozzle, which can create a more even distribution of particles. Afterwards, the particles then enter either a honeycomb type geometry or a series of grooves to force the particles and fluid to flow in the direction of the nozzle, reducing the induced swirling from before.

For the purposes of this study, a dual-coaxial nozzle setup is implemented, with the inner nozzle being used for powder flow, and the outer nozzle being used to supply shielding gas flow. In addition, each nozzle has 4 inlets to supply either powder + carrier gas or shield gas, respectively. Figure 1 shows the geometry of the nozzle used in this paper, which is the base for the design changes shown in Section 4, also outlined in Figure 2. In simulations, this nozzle ejects into open atmosphere to simulate a free-stream environment, which is simulated as a cylinder with a diameter of 50 mm and a height of 50 mm. As this study is concerned with the powder flow characteristics of the nozzle, no cooling apparatus is used for this nozzle geometry.

2.2 Fluid Flow

It has been well established that turbulent modeling is best suited for gas-powder flow [4, 5]. As such, this paper also uses a turbulent model for the CFD simulations presented in this paper. In this case, argon is the fluid of choice for all sections of the domain, whereas the powder material is outlined in section 2.3. Because there is no need to understand how individual powders travel through the nozzle to understand nozzle focusing, a steady-state model is preferred. Although symmetry could be considered with this model, a full 3D model in Cartesian coordinates was chosen in order to best match the actual geometry of the nozzle and account for any possible randomness within the powder trajectories. Therefore, we can use the conservation equations given below [9], With gravity ($g_y = 9.81 m/s$) acting in the negative y direction:

The conservation of mass equation:

$$\nabla \cdot (\rho \vec{v}) = 0 \tag{1}$$

The momentum equation:

$$\rho \vec{v} \cdot \nabla \vec{v} = -\nabla P + \nabla \cdot \bar{\bar{\tau}} + \rho \vec{g} + S_i \tag{2}$$

where $\bar{\bar{\tau}}$ is the stress tensor and given as:

$$\bar{\bar{\tau}} = \mu[(\nabla \vec{v} + \nabla \vec{v^T}) - 2/3 \nabla \cdot \vec{v} I] \tag{3}$$

where μ and ρ are the dynamic viscosity and the density of the continuous argon gas, respectively, P is the gas pressure, $\vec{v}$ is the gas velocity, $\nabla = \frac{\partial}{\partial x} + \frac{\partial}{\partial y} + \frac{\partial}{\partial z}$, and $S_i (i = x, y, z)$ represents the source terms. In this case, the discrete phase has a coupling term to represent the transport of momentum between from the particle phase to the gas phase

$$S_i = \frac{1}{V_{cell}} \sum_{1}^{n_c} \left(\frac{18 \mu C_D Re_p}{24 \rho_p d_p^2} (v_{p,i} - v_i) \right) \dot{m}_p^j \Delta t^j \tag{4}$$

TABLE 2. ALL DESIGN PERMUTATIONS THAT WERE TESTED. EACH DESIGN WAS SIMULATED AT 2 DIFFERENT INLET CONDITIONS: 1 KPA AND 10 KPA FOR BOTH SHIELD AND POWDER INLETS.

Design	Powder Inlet Angle (°)	Inlet Offset (mm)	Grooves (#)	Groove Type
1	0	0	0	None
2	0	10	0	None
3	25	0	0	None
4	25	10	0	None
5	0	0	12	Straight
6	0	10	12	Straight
7	25	0	12	Straight
8	25	10	12	Straight
9	0	0	12	Tapered
10	0	10	12	Tapered
11	25	0	12	Tapered
12	25	10	12	Tapered

where V_{cell} is the volume of a given cell within the mesh; n_c is the total number of particle trajectories passing through the given cell; ρ_p is the particle density; d_p is the particle diameter; $v_{p,i}$is the particle velocity component $(i = x, y, z)$; C_D is the particle drag coefficient; Re_p is the particle Reynolds Number; and $\dot{m}_p^j$ is the particle mass flow rate of a specific trajectory passing through the given control volume.

In this study, the standard $k - \varepsilon$ model was used to model the turbulent flow since it was reported by Wen et al. [5] that it is most commonly used turbulence model in coaxial nozzle simulation. In this model, two variables are introduced to describe the conditions in which turbulence occurs, with the first being turbulent kinetic energy k, and the second being the dissipation rate of the turbulent kinetic energy ε. In a 3D steady sate model, the following equations are used to monitor these values [10]:

The turbulent kinetic energy (TKE) equation:

$$\frac{\partial(\rho k v_i)}{\partial x_i} = \frac{\partial}{\partial x_j}[\frac{\mu_t}{\sigma_k}\frac{\partial k}{\partial x_j}] + 2\mu S_{ij}S_{ij} - \rho\varepsilon \tag{5}$$

The TKE rate of dissipation equation:

$$\frac{\partial(\rho \varepsilon v_i)}{\partial x_i} = \frac{\partial}{\partial x_j}[\frac{\mu_t}{\sigma_\varepsilon}\frac{\partial \varepsilon}{\partial x_j}] + 2C_{1\varepsilon}\frac{\varepsilon}{k}\mu S_{ij}S_{ij} - C_{2\varepsilon}\rho\frac{\varepsilon^2}{k} \tag{6}$$

TABLE 3. FULL FACTORIAL DESIGN FOR THE ANALYSIS OF THE NOZZLE DESIGNS.

Factors	Factor Codes	# of Levels	Levels	Level Values
Inlet Pressure (Pa)	A	2	-1,1	1000, 10000
Inlet Angle (°)	B	2	-1,1	0, 25
Inlet Offset (mm)	C	2	-1,1	0, 10
Groove Type	D	3	-1,0,1	Straight, None, Tapered

where S_{ij} is the fluid strain rate tensor, the total viscosity is defined by $\mu = \mu_l + \mu_t$, μ_l is the laminar viscosity, and $\mu_t = C_\mu k^2/\varepsilon$ is the turbulent viscosity. In addition, there are a total of five constants that have been empirically determined for the standard k-ε model: $C_{1\varepsilon} = 1.44, C_{2\varepsilon} = 1.92, C_\mu = 0.09, \sigma_k = 1.0$, and $\sigma_\varepsilon = 1.3$. The last two constants are the Prandtl numbers for k and ε, respectively.

2.3 Discrete Phase Method

The discrete phase method (DPM) is a Lagrangian-Eulerian approach to a two phase flow, where the Lagrangian phase are discrete powders, bubbles, or droplets, and the Eulerian phase is the fluid flow outlined above. Although both Lagrangian-Eulerian and Eulerian-Eulerian methods are both viable for powder-gas flows, the former is best suited for flows where the discrete phase has a volume fraction less than 10% [11]. Given that most DLD processes have low powder feed rates (1-10 gram/min), it is appropriate to use the discrete phase method.

One of the main benefits of using DPM is the ability to track the position and velocity of the particles within the space over a period of time. In a steady-state solution, this means that the full particle trajectory within the desired space is shown for each tracked particle, allowing for a visual analysis of the focusing quality within the nozzle, where particles accumulate, and how fast are the particles moving at a desired point. In addition, DPM can also evaluate the concentration of particles at a given point, allowing for one to determine where particles will build up within the nozzle, as well as to understand the shape of the particle cloud that exits the nozzle. These two tools combined allow one to obtain insight into how well a nozzle focuses.

The governing equations used for the discrete phase method are as follows:

$$\frac{d\vec{x}}{dt} = \vec{v}_p \tag{7}$$

TABLE 4. P-VALUES FOR THE COMBINATION OF FACTORS WITH RESPECT TO EACH MEASURED PARAMETER.

Source	Max DPM Concentration	Cloud Diameter	Min Particle Velocity	Max Particle Velocity
A	0.833	0.833	**0.000**	**0.000**
B	0.130	0.130	0.368	**0.006**
C	**0.020**	**0.020**	**0.029**	**0.038**
D	**0.016**	**0.016**	**0.007**	**0.001**
A*B	0.330	0.330	0.368	0.095
A*C	0.299	0.299	**0.015**	0.423
A*D	0.491	0.491	**0.007**	**0.002**
B*C	0.191	0.191	0.147	**0.020**
B*D	0.154	0.154	0.037	**0.050**
C*D	**0.029**	**0.029**	**0.009**	0.125
A*B*C	0.364	0.364	1.000	**0.038**
A*B*D	0.448	0.448	0.058	0.250
A*C*D	0.289	0.289	**0.018**	**0.050**
B*C*D	0.183	0.183	0.750	0.500

$$\frac{d\vec{v}_p}{dt} = \frac{18\mu C_D Re_p}{24\rho_p d_p^2}(\vec{v} - \vec{v}_p) + \frac{\vec{g}(\rho_p - \rho)}{\rho_p} \quad (8)$$

$$Re_p = \frac{\rho d_p |\vec{v} - \vec{v}_p|}{\mu} \quad (9)$$

Where Re_p is the relative Reynolds Number C_D is the drag coefficient, ρ, and μ are the fluid density and viscosity, respectively; and ρ_p, d_p, and v_p are the particle density, diameter, and velocity, respectively. For the case of DLD, the main driving forces are gas flow and gravity, with wall collisions only momentarily coming into play. However, the drag coefficients vary depending on the geometry of the particles, such as spherical [12] or nonspherical [13]. In the present study, a spherical drag law was considered due to its simplicity and reduced computational time.

Generally, powders used in the DLD process have a diameter range of 10-100μm [3]. It is possible that a given powder sample may have a distribution of diameters that can be described with a function. To describe this distribution pattern, the Rosin-Rammler distribution method is used. This approach divides the entire range of a given particle distribution to a range of discrete

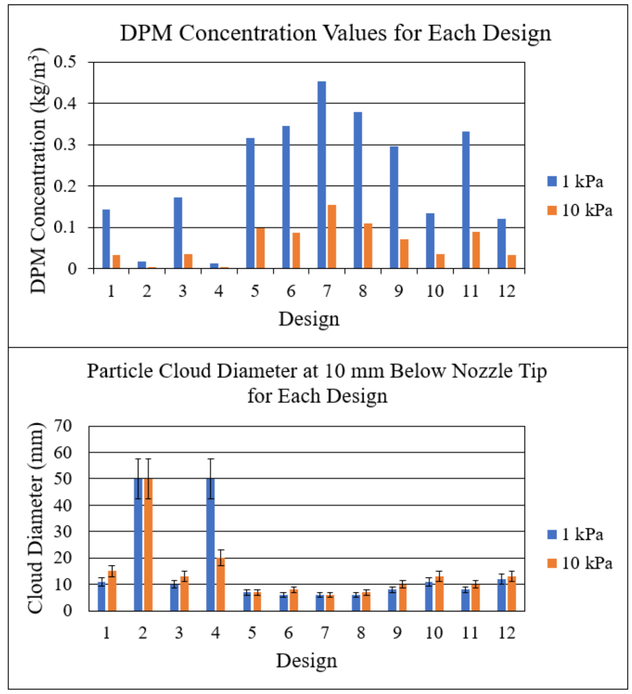

FIGURE 3. A COMPARISON OF ALL DESIGNS AT BOTH INLET PRESSURES (1KPA AND 10KPA) BY EXAMINING SIMULATED PEAK POWDER CONCENTRATION AND PARTICLE CLOUD DIAMETER.

diameters. This distribution function can be given as follows:

$$F_d = exp(-(\frac{d}{\bar{d}})^n) \quad (10)$$

where the function above describes the mass fraction F_d of particles greater than a given particle diameter d. $\bar{d}$ is the average particle diameter, and n is the spread parameter. The material parameters used in the simulations are presented in Table 1.

3 Simulation Setup

A coaxial nozzle works best using low flow-rate inlet conditions or low inlet pressure conditions, which ensures the best focusing at the cost of the ejected powder flow not being fully coaxial. This limitation may be a barrier for proliferation of this technology, as not all facilities will be able to produce proper conditions. Even still, the focusing of a coaxial nozzle could still be improved so that nearly all of the powders will be focused at a specific spot within the beam. Therefore, it is important to explore various design conditions and combinations to determine what enables the best focusing, as well as explore the drawbacks that come from these design changes.

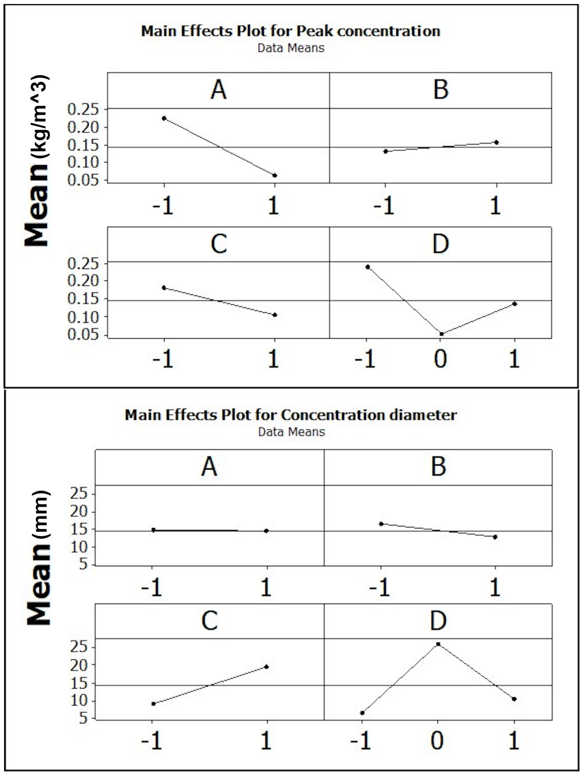

FIGURE 4. MAIN EFFECTS PLOTS GENERATED FROM ANOVA ANALYSIS FOR PEAK CONCENTRATION AND CONCENTRATION DIAMETER.

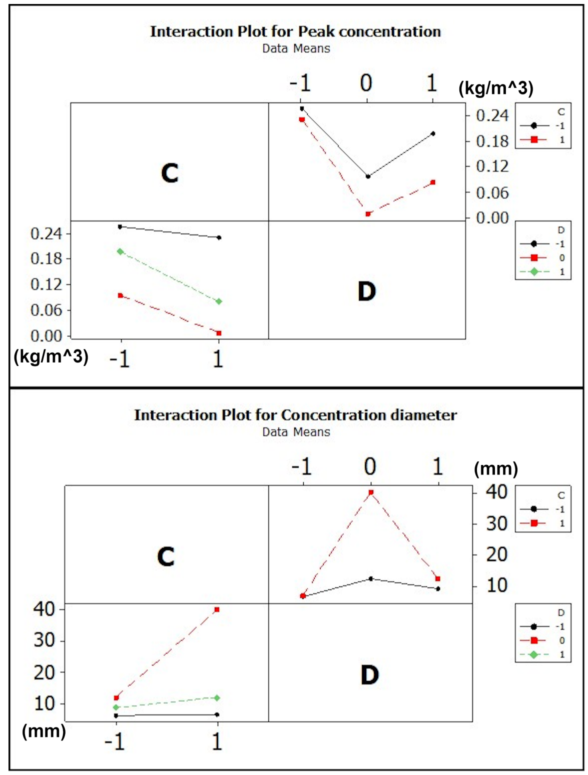

FIGURE 5. INTERACTION PLOTS EXAMINING THE INTERACTION BETWEEN INLET OFFSET AND GROOVE TYPE FOR PEAK CONCENTRATION AND CONCENTRATION DIAMETER.

Given the constraints of the initial design, it was determined that there are 3 specific design aspects that could be implemented without the initial design: nozzle inlet angle, nozzle inlet offset, and the use of a flow straightening mechanism. The angle of the inlets measured from the horizontal plane affects how the powders first enter the main chamber and spread out. Meanwhile, changing the offset of the inlets determine how much tangential velocity is induced into the particle flow initially. This change can also produce a more even particle spread within the system. It is also worth investigating how swirling flow affects particle focusing, and whether or not a there is a need for another correcting feature to stop the swirling flow once the particles are evenly distributed.

This correcting feature is where a flow straightening mechanism can come into play. This can come in the form of a honeycomb or a series of parallel tubes that is nested within the nozzle section. However, such a feature requires an entire section dedicated to it within the nozzle, which would reduce the compactness of the design. Therefore, another feature that achieves a similar result is needed. This can be found in the form of grooves that run down the length of the nozzle, which effectively produces a more compact flow-straightening feature for the nozzles form factor, with the added benefit of only needing to change the geometry of the inner nozzle section shown back in Figures 1 and 2. In addition, the shape of these grooves can be changed, meaning that different groove shapes can be explored. In this study, only three different groove shapes are considered: tapered grooves, straight grooves, and no grooves present. It is important to note that there are technically 5 separate groove cases as the entrance section to the grooves themselves need to account for whether or not the inlets are offset or not. In other words, the groove entrances need to capture the flow of gas and powder in an effective manner and funnel them into the grooves themselves, and therefore need to account for whether or not the flow is swirling and the direction of the swirl.

From all of these features, a total of 12 design combinations are possible based on the full factorial design of experiment. Each design was created in a CAD software (Solidworks 2018) and then the inside volume was meshed as outlined in Section 2.1. From there, each design was simulated in ANSYS Fluent 19.0. However, since it has been shown that the inlet conditions can affect powder focusing, two different inlet conditions were selected: 1 kPa pressure inlets and 10 kPa pressure inlets. Pressure inlets were chosen to reduce computational time for the

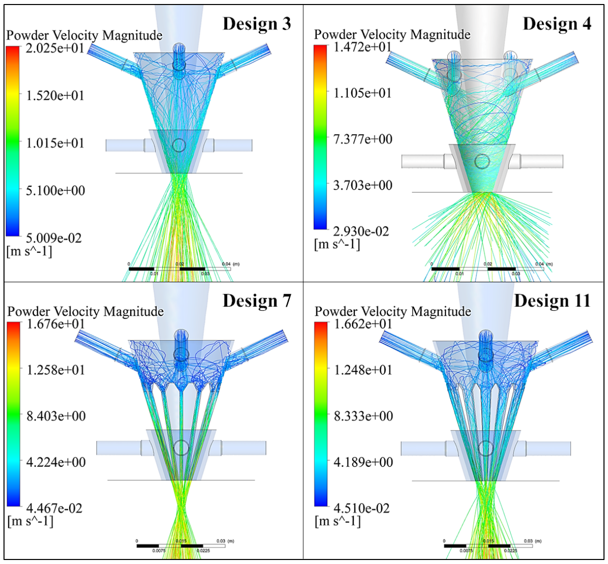

FIGURE 6. PARTICLE TRAJECTORIES FOR EACH MAIN TYPE OF DESIGN.

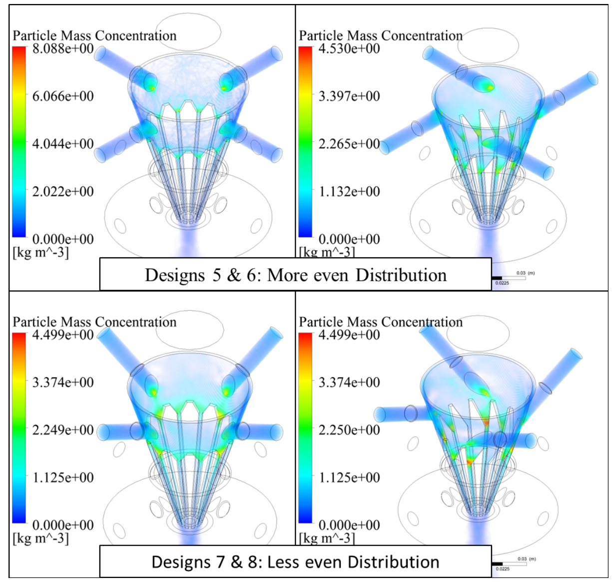

FIGURE 7. DEMONSTRATION OF HOW INLET ANGLE AND OFFSET AFFECTS PARTICLE DISTRIBUTION WITHIN THE NOZZLE.

pressure based solver in fluent, whereas the values were selected to represent both lower and higher flow rate conditions without needing to simulate too many changes in inlet conditions. These conditions now create a total of 24 individual simulations considering two different pressure inlet conditions for each simulation.The design permutations regarding to CFD simulations are outlined in Table. 2.

4 Simulation Results and Discussion

After simulating each design, several parameters were analyzed to determine particle behavior at the focusing region. These included: (i) Peak concentration – the highest powder concentration value obtained from the simulation taken at a plane 10mm below the nozzle using a powder concentration contour map of the plane, (ii) the diameter of the particle cloud – defined to be the diameter measured of the powder concentration contour map at the 10mm plane with a cutoff threshold of 10% of the peak, and (iii) maximum and minimum particle velocity magnitude measured at the 10mm plane. These results were tabulated then grouped up into different design features and analyzed to determine which features or combination of features are the most impactful to the design. The Full Factorial Method was used to analyze the relationship between the input and output parameters, as shown in Table 3. In addition, particle tracing and other simulation plots are obtained from ANSYS and analyzed to determine the behavior of the particles within the nozzle, as well as to verify the underlying mechanisms behind the results.

Through the Full Factorial Method, P-values were obtained for each of the 4 output parameters for each of the initial inputs, as well as their combinations up to 3 factors. Through examination of the P-values in Table 4, it is possible to determine which factors significantly affect the dynamics of the powder spray, with a P-value ≤ 0.05, meaning the factor shows significant effects. For all measured parameters, the inlet offset and type of grooves (factors C and D) show significant effects for all measured parameters, and are the only factors which combination has a P-value less than 0.05 for the focusing parameters (i and ii). As expected, the maximum and minimum particle velocity is affected the most by the inlet pressure, as the inlet conditions determine how the initial flow performs. However, it is apparent that all factors affect the minimum particle velocity in some form, meaning that the relationship is harder to analyze without analysis of the particles through flow simulation.

Although the ANOVA tables are able to demonstrate which factors affect the desired parameters the most, it is hard to determine how that is done without further analysis. Regarding the Focusing parameters (peak concentration and concentration diameter), one way to determine how these two parameters interact is to compare the resulting values between each design and determine patterns. Figure 3 shows the values obtained from the simulation for both focusing parameters, which are measured at 10mm below the nozzle tip. By comparing these charts to Table 2, it is apparent that the designs can be split up into about 5 categories: No grooves and no offset (designs 1 and 3); No grooves and offset present (designs 2 and 4); straight grooves (designs 5-8); tapered grooves without offset (designs 11 and 13); and tapered grooves with offset (designs 12 and 14).

One important thing to note in Figure 3 is the concentration differences between the low and high pressure cases, which is a result of the differing particle velocities. As the average particle velocity increases for any design, the concentration decreases. Essentially, faster moving particles mean that they do not linger in a given space or mesh cell for long before exiting the cell, meaning that the overall concentration at a given instant is lower. This can be confirmed by analyzing the main effects plot for peak concentration, shown in Figure 4.

Designs 1-4 are the designs without grooves, meaning that the overall nozzle geometry represents a typical coaxial nozzle; these designs are split up into the two groups: Straight inlets (1 and 3) and offset inlets (2 and 4). From Figure 3, it is apparent that both the peak DPM concentration and the particle cloud diameter vary drastically from the two groups, with the designs 1 and 3 having relatively average concentration and cloud diameter, and designs 2 and 4 having minimal concentration and extremely high cloud diameter. As the only difference between these two designs is the inlets are offset, meaning this change is due to an additional radial component to the flow for designs 2 and 4.

According to the interaction plots given in Figure 5, specifically the plots where parameters C and D are compared against each other, the nozzle designs corresponding to offsets without grooves have a sizeable dip in the data means for peak concentration, and a significant spike in the concentration diameter. It could be easily confirmed from the particle trajectories generated in Figure 6. Design 3 is in the first group, and although has some spreading of the particles due to some of them accumulating a radial component within the nozzle chamber, it has decent focusing. However, Design 4 is in the second group, and the powder trajectories do not focus at all; instead, they spread out away from the nozzle, following their exit trajectories as there are no nozzle walls or other inwards pointing force to ensure the powder particles follow the swirling flow after exiting the nozzle.

Designs 5-8 all have straight, narrow grooves, and also have the highest peak concentration values, as well as consistently small focusing diameters according to Figure 3. It is this groove shape that predominately ensures that these designs focus so well, since each design does vary in inlet geometry. This can be also confirmed by analyzing Figure 5. Interactions between B and D as well as C and D show that the values corresponding to the -1 factor for D (which corresponds with straight grooves) do not change drastically, if at all. The reason why straight grooves are so effective in improving the nozzle's focusing is because they force all the particles to travel in the desired trajectory, with little to no deviation. As seen in Figure 6, the nozzles similar to Design 7 eliminate any radial component of the particles' velocities, forcing them to travel down towards the focus point of the nozzle. In essence, these nozzles mitigate the radial velocity component, where as designs similar to Design 4 exacerbate it.

Designs 9-12 are split up into two different groups as well in accordance to Figure 3. Designs 9 and 11 have straight inlets, whereas designs 10 and 12 have offset inlets. The tapered grooves do not fully eliminate the radial velocity component like the straight grooves do, which can be seen when comparing Designs 7 and 11 in Figure 6. Instead, the particles bounce between the sides of the grooves, and continue to have a tangential component as they travel through and exit the nozzle. This reduces focusing within the nozzle, and the amount of focusing can be changed by the amount of initial swirling the particles have. Designs 10 and 12 have offset inlets and therefore an initial swirling flow within the nozzle, and as such have a slightly increased focusing diameter and a drastically reduced peak concentration. This is likely because the tangential velocity component is not as easily eliminated in the tapered grooves, and offset inlets induce a larger tangential component in the powder's trajectory. When the powders exit the nozzle they are more likely to exit in a trajectory away from the ideal focus point.

By comparing these two design groups, it is apparent that the direction of the particles' velocity vector greatly affects whether the powder stream will focus or not. If the powders have a tangential velocity component, then there will be spreading. This can be done directly by offsetting the inlets; however, even with straight inlets, the forced reflection of the powders produce varying tangential velocity components for each powder. In order to reduce this velocity component, new geometry such as flow straightening grooves must be added as they direct the powders to follow the grooves path. Straight grooves provide the most abrupt elimination of the tangential component, and therefore are recommended to ensure the powder stream is focused.

Although the measured parameters in the design of experiments give us insight on the end results of the nozzle flow, only CFD analysis can give us an insight as to how design parameters influence powder flow within the nozzle. This is especially notable when analyzing powder distribution within the nozzle, which in this case is governed by the inlet geometry configurations. As shown in Figure 7, the main factor that affects powder distribution is actually in fact inlet angle, especially in designs such as this where the inner chamber is relatively thin. Specifically, this phenomenon is present only for nozzles with grooves, and isn't greatly impacted by groove shape.

A more horizontal inlet allows for the the powders to spread out more as they hit the inside wall of the nozzle's chamber, ensuring that there isn't any bias towards a single groove. However, if the inlets are angled, a larger portion of the powders is biased towards certain grooves over others, meaning that the powder distribution isn't even. If the concentration is too high, there is an increased risk of clogging, inlets ensuring a more even distribution is recommended. It is possible that nozzles with a larger inner chamber or with lower inlet pressures do not ensure that powders will spread in a fashion similar to what these designs experience here, and therefore may also be affected by the presence of offset inlets more so than what the current designs experience.

5 CONCLUSION

In this paper, the design of a DLD nozzle was analyzed through the use of computational fluid dynamics using a dual phase approach. The gas phase was analyzed using an Eulerian-Lagrangian scheme in steady state. It was determined that when the powders enter the nozzle, they collide with the inner wall, then spread out as the space between the nozzle walls are thin. This spreading meant that some of the powder particles produce a tangential velocity component within the nozzle, which will be relatively conserved as the powders travel through the nozzle. This results in reduced powder focusing of a typical coaxial nozzle. It was also determined that higher inlet pressure reduces focusing as the tangential component increases as pressure increases.

The design was then modified to produce a total of 12 distinct designs (24 simulations at 2 distinct pressures),varying parameters such as inlet angle, inlet offset, and inner nozzle geometry (i.e. the presence and shape of flow-straightening grooves). From the analysis of the CFD simulations, it was observed that the inlet offset and the presence and shape of grooves mainly affected focusing, such as peak powder concentration and the diameter of the powder cloud. Without grooves, the flow conditions set by the inlet greatly governed how well the powders focused, with offset inlets that induced a swirling flow within the nozzle producing the greatest amount of spreading. However, with the presence of grooves, the diameter of the powder cloud is reduced. Straight grooves produced the best focusing results, with the powder cloud diameter consistently being around 6-8 mm, and peak powder concentration reaching 0.35-0.45 kg/m^3. Tapered grooves also improved focusing, but to a lesser degree and focusing was still impacted by inlet offset. From the simulations, it can be recommended that future nozzle designs should incorporate straight grooves in order to best improve powder focusing. This is because straight grooves effectively eliminate the tangential velocity component of the powder particles, whereas the tapered grooves do not full eliminate it, instead allowing particles to bounce back and forth between the tapered groove walls.

In addition, the effect of inlet angle was shown to manifest in how the powders were distributed between the grooves. An inlet angle that is more aligned with the angle of the nozzle produced a bias towards grooves that were directly underneath the inlet, whereas a more horizontal inlet allowed the particles to spread out more before they hit the flow-straightening section. It is apparent that the section where the powder is funneled into the grooves produces the highest point of concentration within the nozzle. Although clogging was not considered in this paper, it is possible that this could occur, especially with the straight groove design. As such, future work should consider the effects of clogging and wear within the nozzle. In addition, it is important to note that this paper focuses solely on simulation.Therefore, future work will need to focus on comparing simulation results with experimental results.

ACKNOWLEDGMENT

The authors gratefully acknowledge the financial support provided for this study by Korea Institute of Machinery and Materials (KIMM).

REFERENCES

[1] Sears, J., 2001. "Solid freedom fabrication technologies: Rapid prototyping-rapid manufacturing". *International Journal of Powder Metallurgy,* ***37***(2), pp. 29–30.

[2] Jeantette, F. P., Keicher, D. M., Romero, J. A., and Schanwald, L. P., 2000. Method and system for producing complex-shape objects, Apr. 4. US Patent 6,046,426.

[3] Thompson, S. M., Bian, L., Shamsaei, N., and Yadollahi, A., 2015. "An overview of direct laser deposition for additive manufacturing; part i: Transport phenomena, modeling and diagnostics ". *Additive Manufacturing,* ***Volume 8***, pp. 36–62.

[4] Lin, J., 2000. "Numerical simulation of the focused powder streams in coaxial laser cladding". *Journal of Materials Processing Technology,* ***105***(1-2), pp. 17–23.

[5] Wen, S., Shin, Y., Murthy, J., and Sojka, P., 2009. "Modeling of coaxial powder flow for the laser direct deposition process". *International Journal of Heat and Mass Transfer,* ***52***(25-26), pp. 5867–5877.

[6] Tabernero, I., Lamikiz, A., Ukar, E., de Lacalle, L. L., Angulo, C., and Urbikain, G. "Numerical simulation and experimental validation of powder flux distribution in coaxial laser cladding". *Journal of Materials Processing Technology,* ***210***(15), pp. 2125–2134.

[7] Tabernero, I., Lamikiz, A., Ukar, E., De Lacalle, L. L., Angulo, C., and Urbikain, G., 2010. "Numerical simulation and experimental validation of powder flux distribution in coaxial laser cladding". *Journal of Materials Processing Technology,* ***210***(15), pp. 2125–2134.

[8] Ibarra-Medina, J., and Pinkerton, A. J., 2010. "A cfd model of the laser, coaxial powder stream and substrate interaction in laser cladding". *Physics Procedia,* ***5***, pp. 337–346.

[9] *ANSYS Fluent Theory Guide, Release 19.2, Help System, ANSYS, Inc.*

[10] Launder, B. E., and Spalding, D. B., 1972. *Mathematical models of turbulence*. No. BOOK. Academic press.

[11] *ANSYS Fluent User's Guide, Release 19.2, Help System, Chapter 23: Modeling Descrete Phase, ANSYS, Inc.*

[12] Morsi, S., and Alexander, A., 1972. "An investigation of particle trajectories in two-phase flow systems". *Journal of Fluid Mechanics,* ***55***(2), pp. 193–208.

[13] Haider, A., and Levenspiel, O., 1989. "Drag coefficient and terminal velocity of spherical and nonspherical particles". *Powder Technology,* ***58***(1), pp. 63 – 70.